

Cyanoacetylene Adsorption on Amorphous and Crystalline Water Ice Films: Investigation through Matrix Isolation and Quantum Study

Fabien Borget, Thierry Chiavassa, Alain Allouche, Francis Marinelli, and Jean-Pierre Aycard*

Contribution from the Physique des Interactions Ioniques et Moléculaires, Université de Provence et CNRS, UMR 6633, Boîte 252, Centre de St. Jérôme, F-13397 Marseille Cedex 20, France

Received February 20, 2001

Abstract: The structure and energy properties of the 1:1 complexes formed between cyanoacetylene and H₂O (D₂O) are investigated using FT-IR matrix isolation spectroscopy and ab initio calculations at the MP2/6-31G(d,p) level. Cyanoacetylene adsorption and desorption on amorphous ice film are monitored by FT-IR using the temperature-programmed desorption method. In an argon matrix, two types of 1:1 complexes are observed. The first one corresponds to the NH structure, which involves a hydrogen bond with the terminal nitrogen of cyanoacetylene. The second corresponds to the HO form, which involves a hydrogen bond from the cyanoacetylene to the oxygen of water. This last complex is the more stable ($\Delta E = -8.1$ kJ/mol.). As obtained in argon matrixes, two kinds of adsorption site are observed between HC₃N and ice. The first one, stable between 25 and 45 K is characterized by a ν_{OH} shift similar to the one observed in matrix for the NH complex. The second, stable at higher temperatures (between 45 and 110 K), corresponds to an interaction with the dangling oxygen site of ice and is similar to the HO complex observed in matrix. From theoretical calculations (DFT method combined with a plane wave basis set and ultrasoft pseudopotentials), it is shown that, for this adsorption site, the HC₃N moiety is flattened on the ice surface and stabilized by a long-distance interaction (~ 3 Å) between one dangling OH and the π system of the C \equiv C triple bond. The HC₃N desorption occurs between 110 and 140 K, and the associated desorption energy is 39 kJ/mol. This value is in good agreement with the first principle calculation based on density functional theory and ultrasoft pseudopotentials (34 kJ/mol). These calculations confirm the electrostatic nature of the interaction forces. A small amount of cyanoacetylene is incorporated into the bulk and desorbs at the onset of the ice crystallization near 145 K. In these two kinds of experiments, HC₃N acts as both an electrophilic and a nucleophilic molecule.

Introduction

Up to 120 molecules has been observed in the interstellar medium (ISM). To understand their formation and evolution, numerous theoretical models, which include detailed physical and chemical pathways, have been developed.¹ For these models, experimental data relating to grain surface processes and chemistry in ices are conspicuously absent. The gas–grain interaction, involving heterogeneous reactions on grain surfaces or in the icy mantles, is nevertheless assumed to play an important role for the formation of molecules in the ISM. Effectively, there are vast quantities of water ice in the low-temperature region of the solar system, which have been detected by infrared spectroscopy.² Present on the satellites of the outer planets and on the comets, water ice is also believed to be an important constituent of interstellar dust.² With regard to the pressure and temperature conditions that exist in the ISM, it is reasonably expected that the ice is amorphous. For these reasons, particular interest has been focused on small molecules interacting with amorphous ice surface.³

* To whom corespondence should be addressed. E-mail: aycard@piimsdm3.univ-mrs.fr.

(1) (a) *I.A.U. Symposium 87, Interstellar Molecules*; Andrew, B. H., Ed.; Reidel: Dordrecht, The Netherlands, 1980. (b) *Solid Interstellar Matter: The ISO Revolution*; Les Houches Workshop; d'Hendecourt, L., Joblin, C., Jones, A., Eds.; Springer/EDP Sciences: New York, 1999. (c) Smith, I. W. M.; Rowe, B. R. *Acc. Chem. Res.* **2000**, *33*, 261 and references therein. (d) Barrientos, C.; Redondo, P.; Largo, A. *Recent Res. Dev. Phys. Chem.* **1997**, *1*, 51.

The physical and structural properties of amorphous solid water have been the subject of numerous publications and reviews.^{2,4} From theoretical and experimental studies of ice clusters and microporous amorphous ice, several aspects of the surface of ice have been revealed. Detailed investigations, coupled with computer modeling, have identified three characteristic surface molecules: those with a dangling OH bond, those with a dangling bond not occupied by H, called dangling O, and four coordinated molecules, called s-4, that are distorted

(2) (a) Petrenko, V. F.; Whitworth, R. W. in *Physics of Ice*; Oxford University Press: New York, 1999. (b) Consolmagno, G. J.; Lewis, J. S. In *Jupiter—Studies of the interior, atmosphere, magnetosphere and satellites*; Gehrels, T., Ed.; University of Arizona Press: Tucson, 1976. (c) Rothly, D. A. *Satellites of the Outer Planets*; Clarendon Press: Oxford, U.K., 1992. (d) Blake, D.; Allamendolla, L.; Sandford, S. A.; Hudgins, D.; Freund, F. *Science* **1991**, *254*, 548. (e) Mayer, E.; Pletzer, R. *Nature* **1986**, *319*, 298. (f) Sanford, S. A.; Allamendolla, L. *Icarus* **1988**, *76*, 201. (g) Westly, M. S.; Baragiola, R. A.; Johnson, R. E.; Baratta, G. A. *Nature* **1995**, *373*, 405.

(3) (a) Delvin, J. P. *J. Phys. Chem.* **1992**, *96*, 6185. (b) Rowland, B.; Kadagathur, N. S.; Devlin, J. P. *J. Chem. Phys.* **1995**, *102*, 13. (c) Smith, R. S.; Huang, C.; Wong, E. K. L.; Kay, B. D. *Phys. Rev. Lett.* **1997**, *79*, 909. (d) Tamburelli, I.; Chiavassa, T.; Borget, F.; Pourcin, J. *J. Phys. Chem. A* **1998**, *102*, 423. (e) Couturier-Tamburelli, I.; Chiavassa, T.; Pourcin, J. *J. Phys. Chem. B* **1999**, *103*, 3677. (f) Borget, F.; Chiavassa, T.; Allouche, A.; Aycard, J. P. *J. Phys. Chem. B* **2001**, *105*, 449. (g) Allouche, A.; Couturier-Tamburelli, I.; Chiavassa, T. *J. Phys. Chem. B* **2000**, *104*, 1497. (h) Manca, C.; Allouche, A. *J. Chem. Phys.* **2001**, *114*, 4226.

(4) (a) Scaats, M. G.; Rice, S. A. In *Water. A Comprehensive Treatise*, 1st ed.; Franks, F., Ed.; Plenum Press: New York, 1982. (b) Angell, C. A. *Annu. Rev. Phys. Chem.* **1983**, *34*, 593. (c) Angell, C. A. *Science* **1995**, *267*, 1924.

Table 1. Experimental and Calculated Frequency Shifts (in cm^{-1}) for $\text{CA}\cdots\text{H}_2\text{O}$ Complexes ($\Delta\nu = \nu$ Monomer $- \nu$ Complex)^a

		experimental				theoretical (MP2/6-31G(d,p))					
		monomer	complex (HO)	complex (NH)	$\Delta\nu(\text{HO})$	$\Delta\nu(\text{NH})$	monomer	complex (HO)	complex (NH)	$\Delta\nu(\text{HO})$	$\Delta\nu(\text{NH})$
H_2O	ν_3	3739.4 (2)		3713.9 (100)		25.5	4030.7 (44)	4029.7 (15)	4010.5 (100)	1	20.2
	ν_1	3639.0 (2)		3600.4 (63)		38.6	3891.9 (5)	3895.4 (4)	3878.1 (95)	-3.5	13.8
	ν_2	1589.5 (100)		1597.0 (98)		-7.5	1681.7 (100)	1674.3 (14)	1703.9 (7.1)	7.4	-22.5
HC_3N	ν_1	3315.9 (100)		3312.2 (36)		2.7	3530.0 (100)		3527.6 (62)		2.4
			3218.5 (100)		96.4			3419.2 (100)		110.8	
	ν_2	2268.7 (82)		2273.6 (59)		-4.9	2246.4 (11)		2252.9 (13)		-6.5
			2263.2 (47)		5.5			2241.4 (10)		5	
	ν_3	2076.5 (16)		2066.7 (65)		9.8	2051.8 (6)		2045.2 (6)		6.6
	$2\nu_5$	1318.3 (10)		1327.3 (12)		-9			2058.6 (3)		-6.8
	ν_4						891.1 (0.5)	894.8 (0.0)	898.5 (0.0)	-3.7	-7.4
	ν_5	667.3 (52)	760 (3)		-92.7		611.1 (56)	711.4 (10)		-100.3	
			670.4 (10)		-3.1			617.2 (33)		-6.1	
ν_6	503.5 (15)	506.1 (3)		-2.6		502.8 (1)	512.6 (0.1)	498.6 (0.01)	-9.8	4.2	

^a Normalized intensities are in parentheses.

from the usual tetrahedral symmetry.⁵ In particular, it has been established, through spectroscopic studies, that dangling OH groups are abundant at the surface of both crystalline and amorphous ice.

The first member of the cyanopolyne family (HC_nN , $n = 3, 5, 7, 9, 11$), cyanoacetylene, is an important odd-nitrogen species of the interstellar medium which was discovered by Turner in 1971 using its known rotational spectrum.⁶ It is third in concentration, after N_2 and HCN , as a carrier of nitrogen in the atmosphere of Titan, and it has recently been suggested that HC_3N might be a possible parent of CN emission from comets.⁷

Water and cyanoacetylene are well-known hydrogen bond formers, showing both proton donor and acceptor nature. Cyanoacetylene aggregates, linked by hydrogen bonds, are of interest as conducting polymer precursors.⁸ In the gas phase, the $\text{HC}_3\text{N}\cdots\text{H}_2\text{O}$ complex was studied by microwave spectroscopy.⁹ The complex has a dynamical C_{2v} structure with the acetylenic proton hydrogen bonded to the oxygen of the water.

The purpose of the present work is 3-fold: (1) obtain direct and accurate experiment results for the $\text{HC}_3\text{N}\cdots\text{H}_2\text{O}$ (D_2O) complexes trapped in cryogenic matrix, (2) assess the chemical stability of cyanoacetylene adsorbed on water ice surfaces, and (3) answer the question, "does water act as nucleophilic or as a proton donor molecule in HC_3N complexes". On the basis of these results, we hope to describe the nature of the adsorption sites of HC_3N on amorphous water ice.

Experiments were monitored by FT-IR spectroscopy. Quantum calculations were undertaken to compare the experimental IR spectra with the calculated ones and thus assign observed absorptions and furthermore determine the complex and adsorption site structures.

Experimental Section

H_2O was doubly distilled before use. D_2O (99.8%) was supplied by SDS and used without further purification. Water and D_2O was degassed by successive freeze-thaw cycles under vacuum before each use.

(5) (a) Rowland, B.; Devlin, J. P. *J. Chem. Phys.* **1991**, *94*, 812. (b) Rowland, B.; Kadagathur, N. S.; Devlin, J. P.; Buch, V.; Feldman, T.; Wojcik, M. *J. Chem. Phys.* **1995**, *102*, 8328.

(6) (a) Arnau, A.; Tunon, I.; Silla, E.; Andres, J. M. *J. Chem. Educ.* **1990**, *67*, 205. (b) Turner, B. *Astrophys. J.* **1971**, *163*, L35.

(7) Brockelee-Morvan, D.; Crovisier, J. *Astron. Astrophys.* **1985**, *151*, 90.

(8) Aoki, K.; Kakudate, Y.; Yoshida, M.; Usuba, S.; Fujiwara, S. *J. Chem. Phys.* **1989**, *91*, 778.

(9) Omron, R. M.; HightWalker, A. R.; Hilpert, G.; Fraser, G. T.; Sueraml, R. D. *J. Mol. Spectrosc.* **1996**, *179*, 85.

Low-density amorphous ice films are obtained from a water/argon (1/50) gaseous mixture deposited on a CsBr window held at 80 K with a 1 nm/s growth rate. The deposition is made under a constant pumping of 10^{-7} mbar in order to outgas Ar and so obtain a porous solid.¹⁰ In addition, the use of a carrier gas allows a best control of the ice deposition. Then the film is recooled to 15 K to deposit pure HC_3N and to study the adsorption process. The microporous^{2c} deposited film thickness is $\sim 0.8 \mu\text{m}$ as deduced from the calibration of infrared absorbance versus film using optical interferences.¹¹ Adsorption and desorption of cyanoacetylene on the amorphous ice film were monitored by infrared spectroscopy using a Nicolet 7199 FT-IR spectrometer in the 4000–400- cm^{-1} wavenumber range at a resolution of 1 cm^{-1} .

Several TPD experiments, adapted to FT-IR spectroscopy as previously described,^{3c} were conducted using different β heating rates. For each of them, we can evaluate the fractional surface coverage from the normalized integrated absorbance of the cyanoacetylene versus T. Above 80 K, during a temperature increase for the TPD experiments, an irreversible modification of the amorphous ice toward a crystalline form was observed near 145 K. Ice retains its crystalline feature, until the sample sublimates at 180 K. This form is characterized by the two shoulders,^{2c} at 3340 and 3150 cm^{-1} , on the large profile of the ν_{OH} mode at 3260 cm^{-1} .

Pure cyanoacetylene was synthesized using the method described by Moureu and Bongrand.¹² The cyanoacetylene is degassed before each deposition. It is trapped in a liquid N_2 /ethanol mixture (115 K) to eliminate N_2 under pumping (10^{-7} mbar) and other impurities such as O_2 and CO_2 . Moreover, the first fraction of cyanoacetylene is evacuated.

The apparatus and experimental techniques used to obtain argon matrixes have been described elsewhere in the literature.¹³ The relative concentrations Ar/ HC_3N (650/1) and Ar/ $\text{HC}_3\text{N}/\text{H}_2\text{O}$ (650/1/20 and 650/1/3.5) at room temperature were adjusted by pressure measurements; reproducible solute partial pressures required the use of a datametric capacitance manometer (Barocel series 600). The mixture was deposited at 20 K on a CsBr window. The deposition rate (2 mmol/h) of gas mixtures was controlled with an Air Liquide microleak (V.P./RX).

Results

1. Study of the $\text{HC}_3\text{N}\cdots\text{H}_2\text{O}(\text{D}_2\text{O})$ Complexes. (a) Cryogenic Matrix Experiments. Argon matrixes containing only HC_3N , H_2O , or D_2O were prepared, yielding infrared adsorption spectra that were similar to those previously reported. Table 1

(10) (a) Givan, A.; Loewenschuss, A.; Nielsen, C. J. *J. Phys. Chem. B* **1997**, *101*, 8696. (b) Givan, A.; Loewenschuss, A.; Nielsen, C. J. *Chem. Phys. Lett.* **1997**, *275*, 98.

(11) Zondlo, M. A.; Onash, T. B.; Warshavsky, M. S.; Tolbert, M. A.; Mallich, G.; Arentz, P.; Robinson, M. S. *J. Phys. Chem. B* **1997**, *101*, 10887.

(12) Moureu, C.; Bongrand, J. C. *Ann. Chim. (Paris)* **1920**, *14*, 47.

(13) Pourcin, J.; Monnier, M. Verlaque, P.; Davidovics, G.; Lauricella, R.; Colona, C.; Bodot, H. *J. Mol. Spectrosc.* **1985**, *109*, 186.

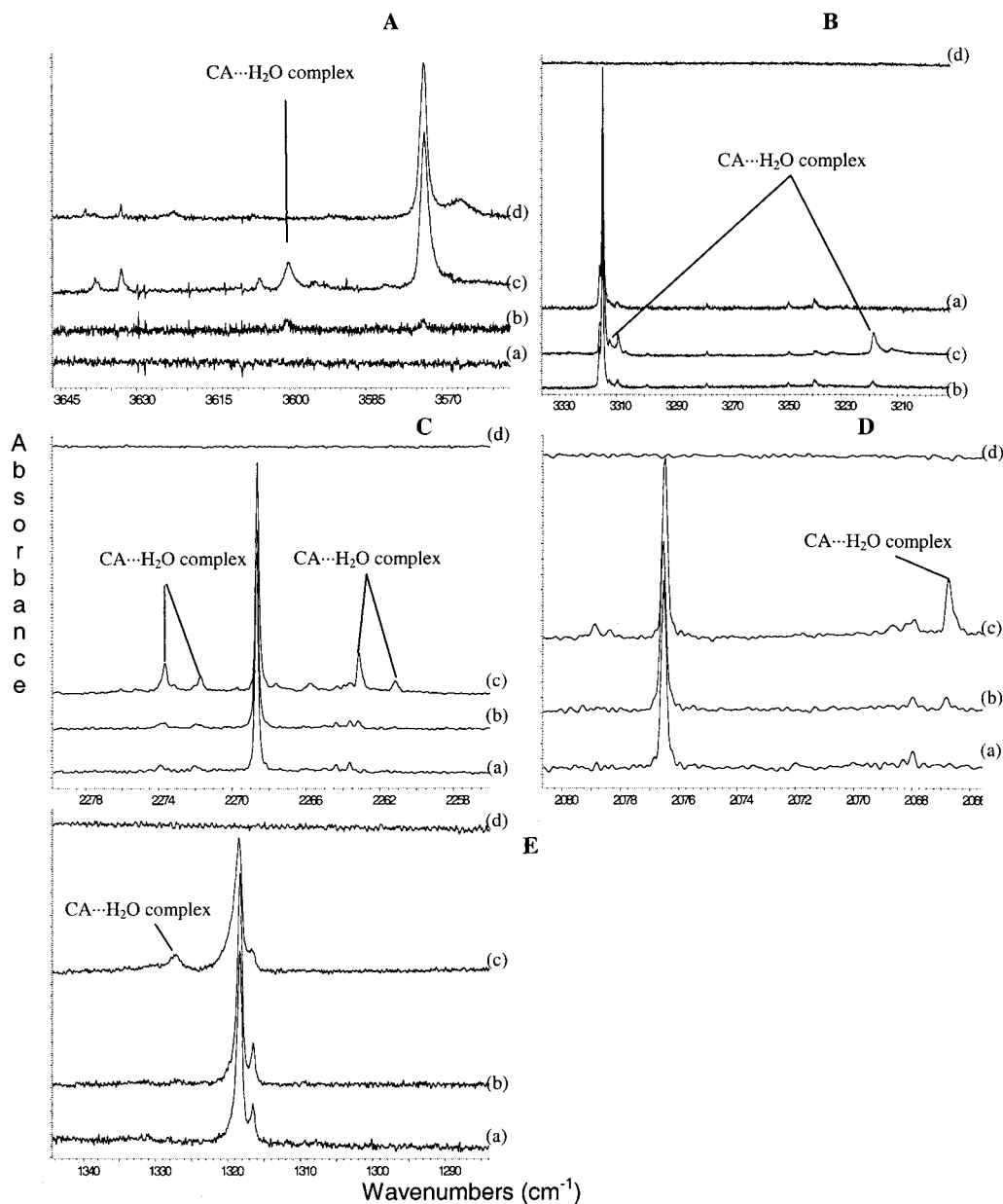


Figure 1. Infrared spectra in different zones at 20 K: (a) CA/Ar 1/650, (b) CA/H₂O/Ar 1/3.5/650, (c) CA/H₂O/Ar 1/20/650, and (d) H₂O/Ar 1/50.

summarizes the observed absorptions with spectral assignments based on the works of Ayers and Couturier-Tamburelli¹⁴ (H₂O, D₂O), Redington¹⁵ (D₂O), and Kolos and Machara¹⁶ (HC₃N). Previous to the adsorption study, matrix isolation experiments were carried out with different compound concentrations. From these experiments, the characteristic absorption bands of free H₂O, (H₂O)_n, and (HC₃N)_n polymers were well identified. The spectra recorded after two co-depositions of H₂O/HC₃N/Ar at 20 K (20/1/650 and 3.5/1/650) show new absorption bands with respect to the spectra of pure H₂O and pure HC₃N trapped in argon matrix (cf. Figure 1 and Table 1).

In the ν_{OH} region, between 3800 and 3450 cm⁻¹ (cf. Figure 1A), we observe the characteristic absorption bands of H₂O monomer and (H₂O)_n polymers. Two absorption bands observed

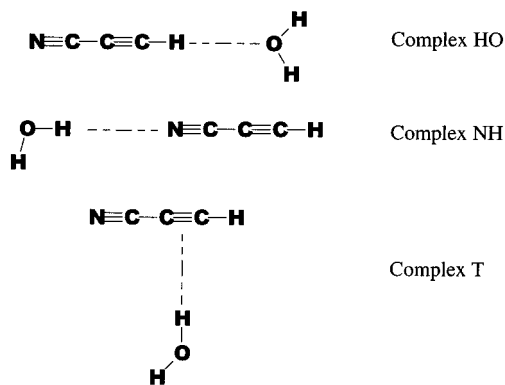
at 3713.9 and 3600.4 cm⁻¹, lower than the value observed for the free ν_{OH} mode, are attributed to the complexes. In the ν_{CH} area between 3450 and 3000 cm⁻¹ (cf. Figure 1B), two new absorption bands appear at 3218.5 and 3312.2 cm⁻¹, corresponding to the ν_1 mode of complexed HC₃N. These values are shifted to the lower frequencies by 96.4 and 2.7 cm⁻¹ with respect to the more intense ν_1 absorption band of the two characteristic sites of pure HC₃N (3315.9 and 3314.9 cm⁻¹). The intensity of the 3312.2 cm⁻¹ absorption band is very weak.

In the ν_2 area (cf. Figure 1C), two doublets, attributed to two sites, appear at 2263.2, 2261.1 cm⁻¹ and 2273.6, 2271.7 cm⁻¹. The more intense band of the first doublet, at 2263.2 cm⁻¹, is shifted to lower frequencies by 5.5 cm⁻¹ with respect to the free $\nu_{\text{C=N}}$ frequency value. The second one, at 2273.6 cm⁻¹, is shifted to higher frequencies by 4.9 cm⁻¹. For the ν_3 ($\nu_{\text{C=C}}$) absorption mode, only one new absorption band is observed at 2066.7 cm⁻¹ (cf. Figure 1D); it is shifted to lower frequencies by 9.8 cm⁻¹ with respect to the ν_3 of pure HC₃N (2076.5 cm⁻¹). Between 1750 and 1500 cm⁻¹ in the $\delta\text{H}_2\text{O}$ region, one new absorption band appears; it is attributed to the ν_2 of H₂O and

(14) (a) Ayers, G. P.; Pulling, D. E. *Spectrochim. Acta* **1976**, *32A*, 1629. (b) Ayers, G. P.; Pulling, D. E. *Spectrochim. Acta* **1976**, *32A*, 1695. (c) Couturier-Tamburelli, I.; Chiavassa, T.; Aycard, J. P. *J. Am. Chem. Soc.* **1999**, *121*, 3756.

(15) Redington, R. L.; Milligan, D. J. *Chem. Phys.* **1963**, *39*, 1276.

(16) (a) Kolos, R.; Waluk, J. *J. Mol. Struct.* **1997**, *408/409*, 473. (b) Machara, N. P.; Ault, B. S. *J. Phys. Chem.* **1988**, *92*, 6241.

Chart 1 Start Positions for Theoretical Calculations of the Complexes

shifted by 3.8 cm^{-1} to higher frequencies at 1597 cm^{-1} . For the first harmonic of the ν_5 mode, two new bands attributed to the 1:1 complexes are observed at 760.0 and 670.4 cm^{-1} , while the ν_6 mode is shifted to higher frequencies by 2.6 cm^{-1} .

The spectrum recorded after co-deposition of $\text{D}_2\text{O}/\text{HC}_3\text{N}/\text{Ar}$ at 20 K shows the characteristic absorption bands of H_2O , HDO , and D_2O species.⁴ The shifts of cyanoacetylene modes in the $\text{D}_2\text{O}\cdots\text{HC}_3\text{N}$ species appear at the same frequencies as in the previous experiments (cf. Table 1).

(b) Quantum Chemistry Results. Our experimental results are indicative to the formation of different 1:1 complexes in the matrix. To establish their molecular structure, ab initio calculations were carried out with Gamess^{17a} and then Gaussian 98^{17b} at the MP2/6-31G(d,p) level of theory.¹⁸ Several arrangements are possible in the H_2O and HC_3N subunits in the complexes. Water and cyanoacetylene are both simultaneous proton donor and acceptor compounds. Water and HC_3N are expected to form hydrogen bonds to nitrogen or oxygen, respectively. Three kinds of complexes are thus considered for optimization and vibrational frequency calculations (cf. Chart 1): the NH form, which involves a hydrogen bonding with the terminal nitrogen of cyanoacetylene, the HO form, which involves a hydrogen bonding with the oxygen of water, and the T form, which involves a hydrogen bonding with the π system of the $\text{C}\equiv\text{C}$ bond.

Geometries of the Complexes (cf. Table 2). Starting from these initial approximations, all the geometrical parameters were fully optimized using the Berny optimization procedure.¹⁹ The harmonic vibrational frequencies were determined at the stationary points and compared to experimental data.

For the $\text{HC}_3\text{N}\cdots\text{H}_2\text{O}$ complexes, calculations give only two local minimums. The first one, with a C_s symmetry structure and with a $r_{\text{N}\cdots\text{H}}$ value of 2.189 \AA , corresponds to the NH structure. The second, with a C_{2v} structure, corresponds to the

(17) (a) Schmidt, M. W.; Baldrige, K. K.; Boatz, J. A.; Elbert, S. T.; Gordon, M. S.; Jensen, J. J.; Koseki, S.; Matsunaga, N.; Nguyen, K. A.; Su, S.; Windus, T. L.; Dupuis, M.; Montgomery, J. A. *J. Comput. Chem.* **1993**, *14*, 1347. (b) *Gaussian 98*, Revision A.7. Frisch, M. J.; Trucks, G. W.; Schlegel, H. B.; Scuseria, G. E.; Robb, M. A.; Cheeseman, J. R.; Zakrzewski, V. G.; Montgomery, J. A., Jr.; Stratmann, R. E.; Burant, J. C.; Dapprich, S.; Millam, J. M.; Daniels, A. D.; Kudin, K. N.; Strain, M. C.; Farkas, O.; Tomasi, J.; Barone, V.; Cossi, M.; Cammi, R.; Mennucci, B.; Pomelli, C.; Adamo, C.; Clifford, S.; Ochterski, J.; Petersson, G. A.; Ayala, P. Y.; Cui, Q.; Morokuma, K.; Malick, D. K.; Rabuck, A. D.; Raghavachari, K.; Foresman, J. B.; Cioslowski, J.; Ortiz, J. V.; Baboul, A. G.; Stefanov, B. B.; Liu, G.; Liashenko, A.; Piskorz, P.; Komaromi, I.; Gomperts, R.; Martin, R. L.; Fox, D. J.; Keith, T.; Al-Laham, M. A.; Peng, C. Y.; Nanayakkara, A.; Gonzalez, C.; Challacombe, M.; Gill, P. M. W.; Johnson, B.; Chen, W.; Wong, M. W.; Andres, J. L.; Gonzalez, C.; Head-Gordon, M.; Replogle, E. S.; Pople, J. A.; Gaussian, Inc., Pittsburgh, PA, 1998.

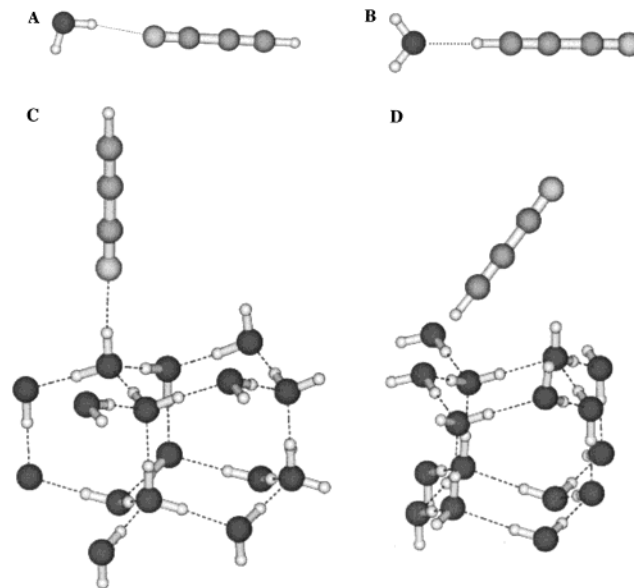
(18) Möller, C.; Plesset, M. S. *Phys. Rev.* **1934**, *46*, 618.

(19) Schlegel, H. B. *J. Comput. Chem.* **1984**, *3*, 214.

Table 2. Geometrical Parameters Calculated for $\text{CA}\cdots\text{H}_2\text{O}$ Complexes at the MP2/6-31G(d,p) Level of Theory^a

	HC_3N	H_2O	$\text{H}_2\text{O}\cdots\text{HC}_3\text{N}$ HO position	$\text{HOH}\cdots\text{NC}_3\text{H}$ NH position
rN1C2	1.188		1.188	1.186
rC2C3	1.377		1.376	1.376
rC3C4	1.223		1.225	1.223
rC4H5	1.064		1.072	1.064
rO6H7		0.961	0.961	0.964
rO6H8		0.961	0.961	0.961
αH7O6H8		103.9	104.9	103.4
dHO			2.057	
dNH				2.189
$\Delta\text{E BSSE (kJ/mol)}$			-20.8	-14.0

^aAll the distances are in angstroms and the angles in degrees.

**Figure 2.** Optimized structures of cyanoacetylene interacting with water as obtained by ab initio calculations: (A) NH position dimer, (B) HO position dimer, (C) NH structure with periodical structure of ice, and (D) HO structure with periodical structure of ice.

HO form ($r_{\text{O}\cdots\text{H}} = 2.057\text{ \AA}$). The T-shaped structure does not correspond to a local minimum. The optimized structures of the complexes with bond lengths are reported in Figure 2A and B and in Table 2.

Identification of the Complexes. The previous calculation provides valuable insight into the stability and the spectroscopic features of the complexes. First, the complexing effects can be observed on the geometry of the partner molecules (cf. Table 2) and on their most significant stretching frequencies (cf. Table 1). By comparison of the ν_{CH} , ν_{CC} , and ν_{CN} vibrational frequency shifts of the complexes with those calculated for the free HC_3N , we are able to identify the forms present in argon matrixes (cf. Table 1).

In the case of the HO complex, for the ν_{CH} (ν_1) and δ_{CCH} (ν_5) modes of cyanoacetylene, large frequency shifts toward lower frequencies are calculated in agreement with an acetylenic hydrogen atom attack on the oxygen of H_2O . The NH form is characterized by weak shifts of the HC_3N absorption bands to higher frequencies and by large H_2O frequency shifts to lower frequencies (cf. Table 1) in agreement with a water hydrogen attack on the nitrogen of HC_3N . These results are compatible with the presence of a HO and NH-shaped structures in the matrix. The intensities' absorption bands of the HO structure are higher than the NH ones in agreement with their calculated energy values (-20.8 and -14.0 kJ/mol for the HO and the

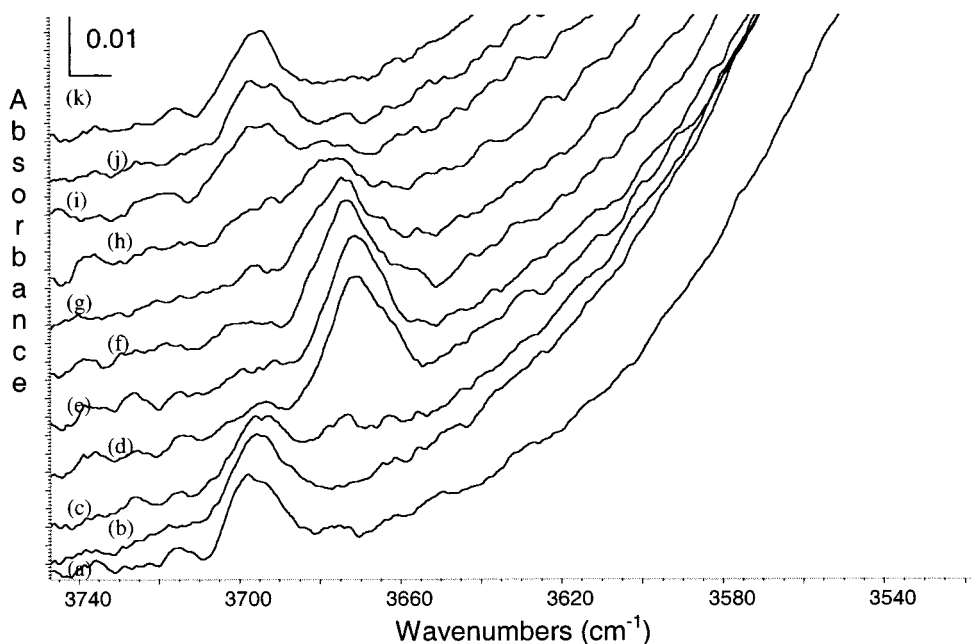


Figure 3. Dangling OH mode region for 0.8 μmol of cyanoacetylene deposited on amorphous ice at 15 K during TPD (0.5 K/min): (a) pure ice at 15 K, (b) 15 K just after cyanoacetylene deposition, and (c) 20, (d) 25, (e) 35, (f) 45, (g) 50, (h) 55, (i) 65, (j) 75, and (k) 80 K.

Table 3. Cyanoacetylene Vibrational Frequency (cm^{-1}) in Argon Matrix Deposited at 20 K and for Solid Deposited at 50 K

mode	argon matrix (1/650) 20 K	solid 50 K	assignment
$\nu_1 + \nu_5$		3958	
ν_1	3314.9, 3315.9	3203	νCH
$\nu_2 + \nu_4$		3137	
ν_2	2268.7	2272	νCN
ν_3	2076.5	2066	$\nu\text{C}\equiv\text{C}$
$2\nu_5$	1318.3	1494	
ν_4		883	$\nu\text{C}-\text{C}$
ν_5	667.3, 665.7	759	δCCH
ν_6	503.5, 502.1	505	δCCN

NH structures, respectively). These results are similar to the ones observed in the gas phase by microwave spectroscopy.⁹ Legon and Millen²⁰ explained that the observation of HO versus NH complexes is due to the limiting gas-phase nucleophilicity value for water, which is significantly larger than its electrophilicity value. For this, dimers of the type $\text{H}_2\text{O}\cdots\text{HX}$ predominate in the observations made so far. For example, it is the case for $\text{C}_2\text{H}_2\cdots\text{OH}_2$,²¹ $\text{HCN}\cdots\text{OH}_2$,^{22,23} and $\text{HCCCCCH}\cdots\text{OH}_2$ ²⁴ dimers.

2. HC_3N on Ice Surfaces. (a) Adsorption–Desorption Experiments. HC_3N adsorption at 15 K on amorphous ice surface induces a slight broadening but no change in the position of the infrared ice absorption bands. The line shape and position of the HC_3N modes are the same as those observed for the solid cyanoacetylene²⁵ (cf. Table 3). After annealing at 25 K, a significant shift of the dangling OH to lower frequencies ($\Delta\nu_{\text{OH}} = 25 \text{ cm}^{-1}$) appears. This shift demonstrates that HC_3N diffusion occurs on the amorphous ice and remains the same between 25 and 45 K. Increasing the temperature to 80 K

induces a decrease of the shifted ν_{OH} absorption band (3670 cm^{-1}) and an increase of the free dangling OH absorption band (3695 cm^{-1}). At 80 K, the intensity of the free ν_{OH} is the same as the one observed before HC_3N adsorption (cf. Figure 3). During this annealing, the intensity of the HC_3N modes remains constant and we observe a weak shift of the ν_{CN} and ν_{CC} absorption modes to lower frequencies, 6.6 and 4.0 cm^{-1} , respectively (cf. Figure 4). These modifications of the infrared spectrum, reported in Figures 3 and 4, are not observed during annealing of pure solid HC_3N between 20 and 80 K and are characteristic of a modification of the adsorption site on the ice surface. This result is indicative of the existence of two kinds of adsorption sites. The first one, stable between 25 and 45 K and characterized by a ν_{OH} shift, indicates an interaction with the dangling OH group; the second, stable at higher temperatures (between 45 and 110 K), corresponds to an interaction with the dangling oxygen sites. It is characterized by a shift to the lower frequencies of the ν_{CN} and ν_{CC} absorption bands similar to the ones observed in matrix for the HO complex. Under HC_3N adsorption, the observed shift for the dangling OH mode (25 cm^{-1}) is similar to that observed under N_2 adsorption (22 cm^{-1}).^{26,27} Nevertheless, the temperature desorption ranges do not correspond. Indeed it is well known that N_2 rapid desorption under vacuum occurs near 60 K,²⁶ whereas cyanoacetylene adsorption modification begin from 45 K (cf. Figure 3).

To confirm the nature of the adsorption sites above 45 K, and to discriminate among the different adsorption sites evoked in the former section, we have adsorbed gaseous O_3 , followed by cyanoacetylene, on ice at 45 K. O_3 is used because on amorphous ice it interacts essentially with the dangling OH sites^{3f} and plays the role of dangling OH site inhibitor. The infrared spectrum analysis shows that the HC_3N line shapes are the same as those previously reported for HC_3N deposited on ice without O_3 . This result confirms that HC_3N interacts with the dangling O sites.

(20) Legon, A. C.; Millen, D. J. *Chem. Soc. Rev.* **1992**, 71.

(21) Peterson, K. I.; Klemperer, W. *J. Chem. Phys.* **1984**, 80, 3073.

(22) Fillery-Travis, A. J.; Legon, A. C.; Willoughby, L. C. *Chem. Phys. Lett.* **1983**, 98, 369.

(23) Heikkilä, A.; Pettersson, M.; Khriachtchev, L.; Räsänen, M. *J. Phys. Chem. A* **1999**, 103, 2945.

(24) Ohshima, Y.; Endo, Y. *J. Chem. Phys.* **1990**, 93, 6256.

(25) Dello Russo, N.; Khanna, R. K. *Icarus* **1996**, 123, 366.

(26) Rowland, B.; Fisher, M.; Devlin, J. P. *J. Chem. Phys.* **1991**, 95, 1378.

(27) Devlin, J. P. *Physics and Chemistry of Ice*; Maeno, N., Hondoh, T., Eds.; Hokkaido University Press: Sapporo, Japan, 1992; p 183.

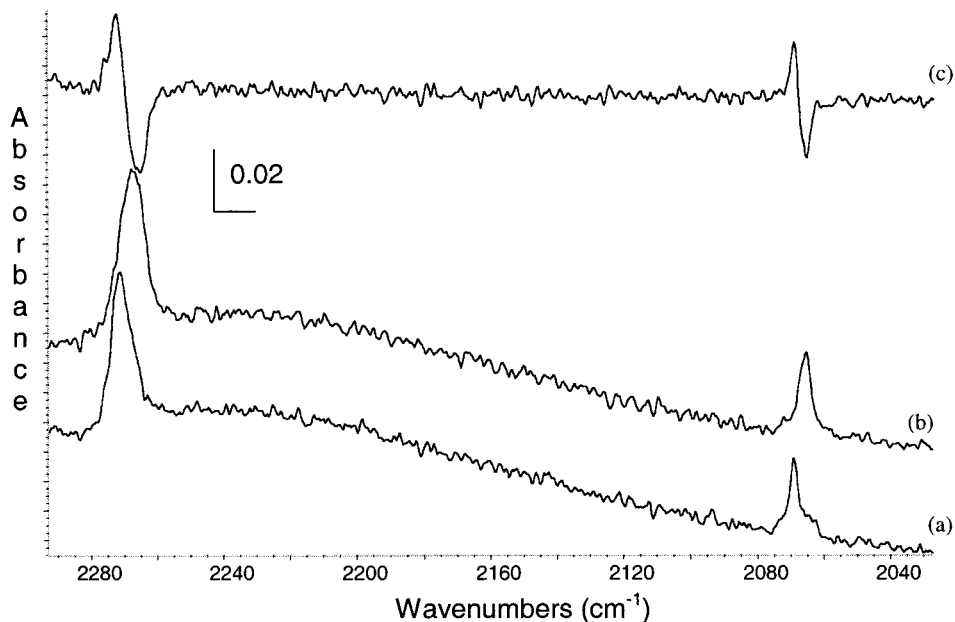


Figure 4. ν_2 and ν_3 cyanoacetylene modes recorded during cyanoacetylene deposition on amorphous ice surface at (a) 25 and (b) 70 K. Spectrum c is the difference spectrum (b) - (a). In positive, cyanoacetylene adsorbed on dangling OH, and in negative, cyanoacetylene adsorbed on dangling O.

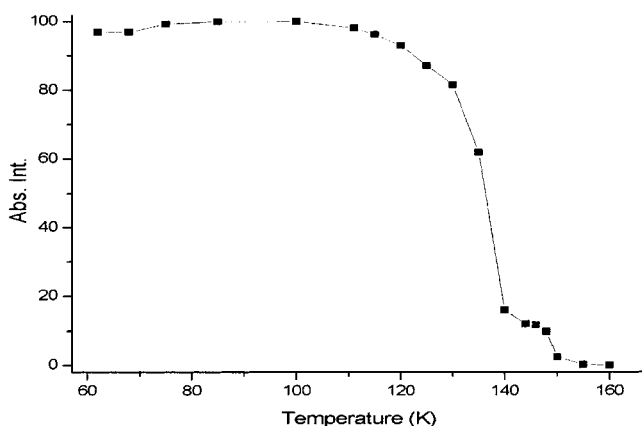


Figure 5. Integrated normalized absorbance of cyanoacetylene ν_2 mode with temperature ($\beta = 0.5$ K/min) for $0.8 \mu\text{mol}$ of cyanoacetylene deposited at 60 K on amorphous ice.

After desorption at 140 K,²⁸ a residual amount of HC_3N , which remains constant in intensity from 140 K to near 145 K, is observed (cf. Figure 5). This result indicates that a small part of the HC_3N is trapped into the ice bulk.

The HC_3N desorption of the dangling O sites follows a first-order kinetic model as displayed in the linear plotting of $\ln \theta = f(T)$ in Figure 6. To characterize the interaction energy between HC_3N and amorphous ice surface, we performed a TPD study monitored by infrared spectroscopy^{3f} between 110 and 140 K. Four experiments were conducted using different β heating rates in the range 0.3–0.8 K/min. As a result, the temperature T_p , for which the desorption is maximal, is evaluated (Table 4) for each heating rate. From the linear plotting of $\ln(\beta/RT_p^2)$ versus $1/T_p$ (cf. Figure 6), $E_d = 39 \pm 8$ kJ/mol. and $A_d = 3 \times 10^{12} \text{ s}^{-1}$ are found.

To complete these experiments, we have also deposited HC_3N at 80 K on an annealed ice film at 165 K. The HC_3N infrared

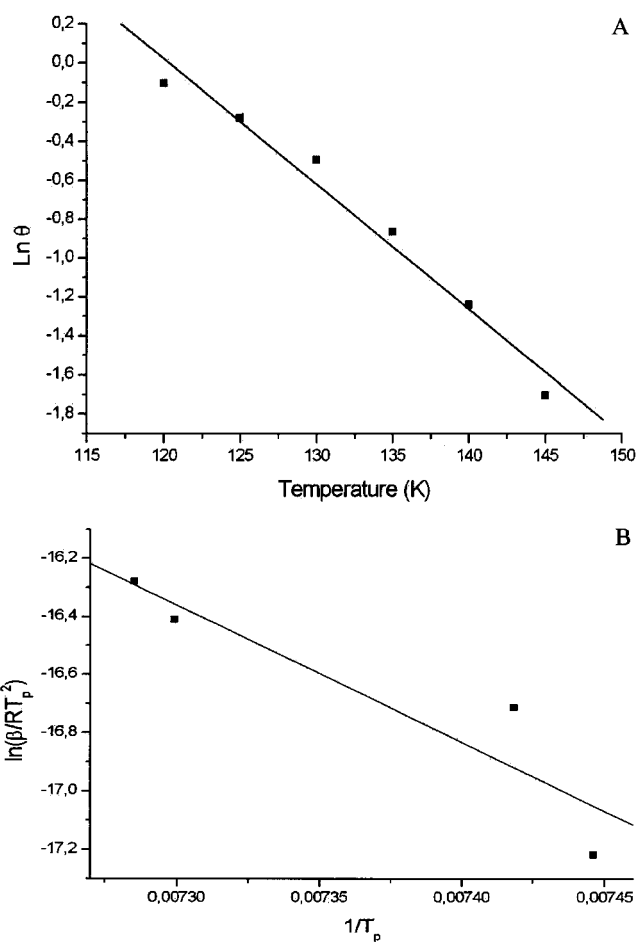


Figure 6. TPD results: (A) experimental points of $\ln \theta$ versus T for $\beta = 0.5$ K/min estimated through the integrated absorbance of ν_2 mode of cyanoacetylene with its linear fit; (B) plot of $\ln(\beta/RT_p^2)$ versus $1/T_p$ for four TPD experiments with its linear fit.

(28) Solid cyanoacetylene fully desorbs at 150 K for the same heating rate (0.5 K/min). It means that interaction between molecules of cyanoacetylene are more important in the solid than when this molecule is adsorbed on an ice surface.

spectra recorded in this case during a TPD experiment show the same evolution as the ones obtained on an amorphous ice surface. This indicates that the adsorption process on amorphous

Table 4. Cyanoacetylene Desorption Peak Maximum Temperature (T_p) for Various Heating Rates (β)

heating rate (K/min)	T_p (K)
0.3	134.3
0.5	134.8
0.7	137.0
0.8	137.3

or crystalline ices is the same. For crystalline ice desorption experiments we do not observe trapping of HC_3N into the ice bulk.

(b) Quantum Results. The reactivity of the surfaces of solids can be studied through different approaches. The Turin group has proposed a very fruitful model for water ice surface based on the periodic Hartree–Fock method (PHF).²⁹ This model is known as the P-ice structure,³⁰ the (001) face is represented by a two-layer slab. Unfortunately, the automatic gradient calculation is not implemented yet in the current version of CRYSTAL98,³¹ the computer program associated with PHF.

An alternative method is the density functional theory (DFT) combined with a plane-wave basis set and with the ultrasoft pseudopotential method as implemented in CASTEP (Cambridge Serial Total Energy Package).³² The density functional we used in the generalized gradient approximation (GGA) is the Perdew–Wang formulation (PW91)³³ which is well known to give very good results on H-bonded systems.

The cell parameters in CRYSTAL98 for the 2D two-bilayers slab are 7.920 and 4.402 Å. They become 7.949 and 4.440 Å after CASTEP optimization. In the PHF approximation, the dangling OH bond length is 0.933 Å and becomes 0.971 Å within DFT. The other OH bond of the same water molecule is also lengthened from 0.970 to 1.026 Å. This general trend is not surprising since it is well known that the DFT leads to larger bond lengths than the HF theory.

On the contrary, the DFT–PW91 calculation gives shorter H-bonds: 1.612 and 1.762 Å in place of 1.747 and 1.816 Å. Nevertheless, these alterations are not dramatic, and since the hydrogen bonds seem well represented, the study of the adsorption of the cyanoacetylene molecule can be investigated on this slab model.

Due to the large size of the HC_3N molecule (~ 4.78 Å) compared to the unit cell parameters, we proceeded with a double supercell whose parameters are 7.490 and 8.869 Å. Two stable structures are found: (i) HC_3N upright above a dangling OH corresponding to a total energy of -304.735435 hartrees and an adsorption energy of 24 kJ/mol. The $\text{HC}_3\text{N}\cdots\text{H}$ distance is 1.965 Å. This distance and the interaction energy are characteristic of a strong hydrogen bond where HC_3N is proton acceptor. (ii) The structure displayed in Figure 2D corresponds to a proton donor role for the HC_3N molecule. The total energy is -304.739299 hartrees, and the adsorption energy is 34 kJ/mol. The stability of this complex is assured by a strong

hydrogen bond between the cyanoacetylene and the dangling lone pair of electrons of an oxygen atom on the ice surface. The associated $\text{H}\cdots\text{O}$ distance is 2.088 Å, and the $\text{C}-\text{H}\cdots\text{O}$ angle is 169.5° .

Discussion and Conclusion

The present study shows that HC_3N is stable on ice below 110 K, which is consistent with interstellar medium conditions ($T < 150$ K). The evolution of the integrated absorbances of the infrared bands shows that cyanoacetylene desorbs from amorphous ice surface in the 110–140 K range of temperature. However, there remains a small amount of HC_3N (5–10%) that is trapped into the bulk up to 145 K. When HC_3N is deposited on an annealed ice film, which is less porous, it is not trapped. This absorbed phase desorbs at the onset of ice crystallization, probably during the nucleation and growth of crystalline ice.

The analysis of our results shows that HC_3N , trapped in cryogenic matrix or adsorbed on an amorphous ice surface, is both electrophilic, by means of its ethynic hydrogen atom, and nucleophilic, by means of the nitrogen atom of its cyano group. For this reason, two kinds of complexes (adsorption sites, respectively) are obtained, both of which are stabilized by hydrogen bonds. The first one corresponds to the NH form and involves a hydrogen bond between the hydrogen atom of water (the dangling OH of ice surface, respectively) and the nitrogen atom of HC_3N . The second one, the more stable, corresponds to the HO form and involves a hydrogen bond between the ethynic hydrogen atom of HC_3N and the oxygen atom of water (the dangling O on the ice surface, respectively).

In all cases, the hydrogen bonds in the HO forms are shorter than in the NH structures and the geometries of the HC_3N moiety are quite similar to those of the free molecule. In the HO forms, we observe a slight lengthening of the CH bond ($\Delta l \approx 0.01$ Å), and in the case of the NH structure, a very weak shortening of the CN bond ($\Delta l \approx 0.001$ Å). These results indicate that the ice crystal field is not in fact of fundamental importance for the HC_3N –ice interactions and that HC_3N interacts weakly with the surface.

For the dangling O adsorption site, the cyanoacetylene is flattened on the ice surface and stabilized by a new long-distance interaction (3.001 Å) between a dangling OH and the π system of the $\text{C}\equiv\text{C}$ triple bond (cf. Figure 2). The calculated adsorption energy ($34 \text{ kJ}\cdot\text{mol}^{-1}$) is in the same order of magnitude as the experimental one ($39 \pm 8 \text{ kJ}\cdot\text{mol}^{-1}$).

For acetylene adsorption on ice, two sites were also observed,³⁴ for one of them, acetylene also possesses a proton acceptor character. Nevertheless, for this site, the interaction is different from the cyanoacetylene one. Indeed, the interaction for acetylene is a hydrogen bond between one dangling OH of the ice and the acetylene π system; in the cyanoacetylene case, the major part of the interaction is between the nitrogen atom of cyanoacetylene and the dangling OH bond of ice. This difference could explain the different dangling shifts observed experimentally for these two molecules.

The dynamic relaxation character of the ice surface, which can occur during annealing experiments,³⁵ leads to a reduction of the porosity and explains the trapping of small amounts (5–10%) of HC_3N . Thus, as the pores are closing, HC_3N is embedded in the bulk. This absorbed phase desorbs at the onset of ice crystallization. This suggests that cyanoacetylene mol-

(29) Pisani, C.; Dovesi, R.; Roetti, C. *Hartree–Fock ab initio treatment of crystalline systems*; Lecture Notes in Chemistry 48; Springer: Berlin, 1988.

(30) (a) Pisani, C.; Casassa, S.; Ugliengo, P. *Chem. Phys. Lett.* **1996**, 253, 201. (b) Casassa, S.; Ugliengo, P.; Pisani, C. *J. Chem. Phys.* **1997**, 106, 8030.

(31) Saunders: V. R.; Dovesi, R.; Moetti, C.; Causa, M.; Harrison, N. M.; Orlando, R.; Zicovich-Wilson, C. M. *CRYSTAL98 user's manual*; Università di Torino, Turin, Italy, 1998.

(32) Milman, V.; Winkler, B.; White, J. A.; Pickard, C. J.; Payne, M. C.; Akhmatkaya, E. V.; Nobes, R. H. *Int. J. Quantum Chem.* **2000**, 77, 895.

(33) (a) Perdew, J. P.; Wang, Y. *Phys. Rev B* **1986**, 33, 880. (b) Perdew, J. P. In *Electronic Structure of Solids*; Ziesche, P., Eschrig, H., Eds.; Akademik Verlag: Berlin, 1991.

(34) Allouche A. *J. Phys. Chem. A* **1999**, 103, 9150

(35) (a) Laufer, D. Kochavi, E.; Bar-Nun, A. *Phys. Rev. B* **1987**, 35, 9219. (b) Bar-Nun, A.; Dror, J.; Kochavi, E.; Laufer, D. *Phys. Rev. B* **1987**, 35, 2427.

ecules are adsorbed both on the external surface and into the pores of the amorphous ice. Thus, the amount of cyanoacetylene trapped in the pores then became embedded during the annealing of the ice and desorbed only at the onset of ice crystallization.

When cyanoacetylene is adsorbed, it exists in equilibrium between the adsorbed HC₃N and the gas phase over the surface. In this case, our results indicate that the dangling OH adsorption process takes place under kinetic control and that the dangling O site is thermodynamically favored. A small barrier separates the two complexes.

Acknowledgment. The theoretical part of this work was realized with the technical means of “Centre Regional de Competence en Modelisation Moleculaire de Marseille”.

Supporting Information Available: Figure of integrated absorbance of the ν CN mode versus temperature for cyanoacetylene adsorbed on ice. This material is available free of charge via the Internet at <http://pubs.acs.org>.

JA0104498